Am J Cancer Res 2021;11(4):1697-1708
www.ajcr.us /ISSN:2156-6976/ajcr0128259

*Original Article*

# CAN017, a novel anti-HER3 antibody, exerted great potency in mouse avatars of esophageal squamous cell carcinoma with NRG1 as a biomarker

Haiyan Liao[1*], Cheng Zhang[2*], Zuhua Chen[2], Ya Gao[3], Zhongwu Li[4], Lingyu Wang[5], Yanyan Li[2], Lin Shen[2,5], Jing Gao[1]

*[1]National Cancer Center/National Clinical Research Center for Cancer/Cancer Hospital & Shenzhen Hospital, Chinese Academy of Medical Sciences and Peking Union Medical College, Shenzhen 518116, China; [2]Key Laboratory of Carcinogenesis and Translational Research (Ministry of Education/Beijing), Department of Gastrointestinal Oncology, Peking University Cancer Hospital and Institute, Beijing 100142, China; [3]CANbridge Life Sciences Ltd., Beijing 100012, China; [4]Key Laboratory of Carcinogenesis and Translational Research (Ministry of Education/Beijing), Department of Pathology, Peking University Cancer Hospital and Institute, Beijing 100142, China; [5]SIP (Suzhou Industrial Park) LifeLink Oncology Research Institute, Suzhou, China. [*]Equal contributors.*

Received December 14, 2020; Accepted January 25, 2021; Epub April 15, 2021; Published April 30, 2021

**Abstract:** CAN017 (AV-203), a novel anti-HER3 antibody, exerts very promising anti-tumor activities in several human tumor models. The aim of this study was to further investigated the efficacy and possible responsive biomarkers of CAN017 in esophageal squamous cell carcinoma (ESCC) with Chinese characteristics. Two separate cohorts of ESCC patient-derived xenograft (PDX) models including 24 (cohort 1 as training models, from Crown Bioscience Inc.) and 22 (cohort 2 as validating models, from Peking University Cancer Hospital) models, respectively, were used to study the efficacy and safety of CAN017, as well as the correlation of NRG1 expression to the response of CAN017. In cohort 1, all PDX models showed good tolerance to CAN017 and 8 out of 24 (33.3%) PDX models responded to CAN017 with tumor growth inhibition (TGI) ≥70% compared to controls. Furthermore, the efficacy of CAN017 was positively correlated with NRG1 expression and the response rates in cohort 1 were 73% (8/11) versus 0% (0/13) in NRG1 high and low expression models, respectively. These results were also validated in PDX models of cohort 2 indicated as the powerful anti-tumor activity of CAN017 in PDX models with NRG1 high expression. In our study, HER3-targeting therapy was first demonstrated to have potency in inhibiting ESCC tumor growth, and NRG1 served as a predictive biomarker to screen patients in future clinical trials.

**Keywords:** ESCC, anti-HER3 therapy, NRG1, PDX model

## Introduction

The morbidity of esophageal cancer in China is very high with more than half of the global cases (53%) [1], however, it's greatly different from the western countries that more than 95% Chinese cases are histopathologically diagnosed as esophageal squamous cell carcinoma (ESCC) [2]. Moreover, due to the low proportion of patients with early diagnosis and treatment, most of the ESCC patients were diagnosed at a later stage with poor prognosis [3-5]. For patients with advanced ESCC, systematic treatment based on drug therapy is still the main strategy, but almost all new targeted drugs developed for ESCC have been failed except for the newly approved Pembrolizumab for second-line therapy [6-10]. Therefore, it's urgent to develop new drugs to improve the prognosis of ESCC.

For several years, targeted HER (human epidermal receptor) family drugs have been the focus of new drug research and development. As one of the members of HER family, HER3 has its unique biological characteristics such as lacking intrinsic tyrosine kinase activity and forming heterodimer with HER2 rather than forming homodimers followed by the activation of downstream signals [11-13]. Also, as a ligand of

HER3, neuregulin 1 (NRG1) is very important to promote the heterodimerization of HER3 and other HER family members [14] and is identified as a predictive biomarker for HER3 targeting therapy in multiple solid tumors. It was reported that HER3 frequently expressed in several cancers including ESCC and its overexpression was correlated with poor prognosis, as well as the close correlation between NRG1 upregulation with HER3 activation and poor prognosis [15-21]. Although no HER3-targeting therapy was approved for cancer treatment nowadays, new drugs targeting HER3 demonstrated the promising application potential, especially the report of U3-1402 in 2019 ASCO annual meeting.

CAN017, also known as AV-203, is a humanized antibody that plays its role via blocking both ligand-dependent and ligand-independent HER3 signalings [22]. The only one preclinical study showed the strong anti-tumor activity of CAN017 in several human tumor models with NRG1 high expression, but only one ESCC cell line KYSE-150 was contained and explored in this study [23]. Although KYSE-150 cells derived xenograft showed response to CAN017, the definite efficacy and safety of CAN017 in ESCC were unclear. In order to provide reliable evidences for future clinical trials in ESCC, this study was designed to investigate the efficacy, safety, and potential biomarkers of CAN017 using the optimal *ex vivo* mouse avatars (also known as patient-derived xenograft models, PDX models) which were highly consistent with patients.

## Materials and methods

### *Reagents*

CAN017 antibody (Anti-HER3-hIgG1/κ) was kindly provided by CANBridge Life Sciences Ltd. (Beijing, China) and dissolved in saline at a stock concentration of 50 mg/mL, and then stored at 2-8°C until used. Control hIgG (Anti-Hel-hIgG1) was purchased from CrownBio (Jiangsu, China) and stocked at a concentration of 4.8 mg/mL in 4°C once dissolved in saline.

### *In vivo animal studies*

Female BALB/c nude mice and nonobese diabetic/severe combined immunodeficiency (NOD/SCID) mice with 6-8 weeks old (Beijing HFK Bio-Technology Co., LTD, Beijing, China) were used in this study. All procedures related to animal handling, care and treatment were performed under sterile conditions at an specific pathogen free (SPF) facility in accordance of the guidance of the Association for Assessment and Accreditation of Laboratory Animal Care (AAALAC). Two separate cohorts of ESCC patient-derived xenograft (PDX) models were used in this study and the procedure of establishment was described as previous report [24]. A total of 24 PDX models of cohort 1 were established using BALB/c nude mice by Crown Bioscience Inc. and 22 PDX models of cohort 2 were established using NOD/SCID mice in Peking University Cancer Hospital.

When the subcutaneous tumors reached 150~200 $mm^3$, mice were randomly assigned to 3 treatment groups with at least 5 mice per group: (1) vehicle control: received 100 μl PBS; (2) hIgG control: received hIgG at a dose of 20 mg/kg; (3) CAN017 group: received CAN017 at a dose of 20 mg/kg. The mice were treated every 3 days by intraperitoneal injection for 3-5 weeks followed by the sacrifice. The tumor volume and body weight of mice were monitored twice weekly, and the tumor volume was calculated using the following formula: Volume = $(a \times b^2)/2$ where A and B are the long and short diameters of the tumors, respectively. Tumor suppression activity was expressed as tumor growth inhibition (TGI) using the following formula: TGI% = $[1-(\Delta T/\Delta C)] \times 100\%$ ($\Delta T$ represents the tumor volume change of the drug-treated group over the course of treatment, $\Delta C$ represent the tumor volume change of vehicle control group over the course of treatment). In this study, the responder to CAN017 was judged as TGI% ≥70%, otherwise, it was judged as nonresponder.

### *RNAseq for HER3 and NRG1 expression analysis*

Total mRNA was extracted using TRIzol reagent (Invitrogen, CA, USA) from frozen xenograft tissues prior to treatment according to the manufacturer's instructions followed by the evalutation of concentrations using NanoDrop™ spectrophotometer. As described as previously reported [25], RNAseq and subsequent data analysis were performed by Novogene Bioinformatics Institute (Beijing, China) and library preparations were sequenced on a Hi-seq 2500 platform (Illumina) as per manufacturer's

recommendation. STAR v2.5.1b was used to align the raw reads to genome sequences and HTSeq v0.6.1 was used to count the reads numbers and calculate fragments per kilobase of transcript sequence per millions base pairs sequenced (FPKM) of each gene. Gene expression level were measured by $\log_2$ (FPKM+1).

*Quantitative real-time PCR for NRG1 expression analysis*

Total RNAs from formalin fixed paraffin embedded (FFPE) tissues prior to treatment were isolated using RNeasy FFPE kit (Qiagen, Hilden, Germany) followed by the evalutation of concentrations using NanoDrop™ spectrophotometer. After reverse transcription using High Capacity cDNA reverse Transcriptase Kit (Applied Biosystems, Foster City, CA), quantitative real-time PCR analyses were performed using TaqMan Universal PCR master Mix (Applied Biosystems, USA) as previously study [23]. The TaqMan probes were Hs01101538_m1 (Human NRG1) and Hs02758991_g1 (Human GAPDH), and NRG1 expressions were normalized to GAPDH according to the comparative threshold cycle ($C_t$) with at least three repeated times. For correlation analysis, $\Delta C_t$ values which normalized to GAPDH were used as an inversely proportional parameter to assess correlations with activity of CAN017.

*Immunohistochemistry (IHC) analysis for HER3 and NRG1 protein expression*

FFPE sections prior to treatment with 4 micron thickness were performed by IHC staining for evaluation of HER3 or NRG1 expressions. NRG1 (rhNRG1-β1) antibody was purchased from R&D Systems (396-HB-050), antibody to HER3 (#12708) was purchased from Cell Signaling Technology. Sections were incubated with anti-HER3 antibody (diluted at 1:250) and anti-NRG1 antibody (diluted at 1:20) at 4°C overnight, respectively. HER3 and NRG1 scores (scores 0, 1+, 2+, 3+) were interpreted by the professional pathologist based on the reported criteria of HER2 evaluation [26].

*Statistical analysis*

Graphs and statistical analysis were performed using GraphPad Prism 8.0 or SPSS 23.0 in this study. Error bars on growth curves were shown as standard deviations (SDs). Tumor growth differences between groups were compared using repeated measures ANOVA t test. Survival analysis for probability of tumor progression-free mice was performed by the Kaplan-Meier method (log-rank test). The Pearson correlation test was applied to define the associations between NRG1 or HER3 expressions and the efficacy of CAN017. The optimal cut-off point of NRG1 expression was determined as the point at which the Youden index was maximized based on receiver operating characteristic curves (ROC). Statistically significant *P* value was indicated as: $^{**}P < 0.01$; $^{***}P < 0.001$; $^{****}P < 0.0001$; ns, not significant.

## Results

*Confirmation of anti-tumor activity and tolerance of 20 mg/kg CAN017 in ESCC PDX models*

In the previous preclinical study of CAN017, 20 mg/kg CAN017 was confirmed to be good safety and high effectiveness [23]. In order to reconfirm the *in vivo* tolerance and activity of 20 mg/kg CAN017 in ESCC, two ESCC PDX models (ES0199 and ES0195) were selected randomly from cohort 1 and used at first. When subcutaneous tumor volume was about 150 $mm^3$, three groups of each PDX model were given vehicle control, 20 mg/kg hIgG, and 20 mg/kg CAN017, respectively, every three days for 3-5 weeks. Good tolerance and safety were found in two PDX models, as evidenced by their clever action and stable body weight (**Figure 1A**). Moreover, 20 mg/kg CAN017 demonstrated different anti-tumor activity in these two PDX models (**Figure 1B**). It was striking that the anti-tumor activity of CAN017 in ES0199 model was very strong with TGI of 105.92%. At the end of drug treatment, the probability of tumor progression-free mice in ES0199 was significant higher than that in ES0195 (**Figure 1C**), which suggested high anti-tumor activity of CAN017 could inhibit tumor progression.

*CAN017 exerted a very promising efficacy in large sample PDX models*

The definite anti-tumor activity of CAN017 was further explored in other 22 ESCC PDX models of cohort 1 based on the results above. All PDX models were tolerant to CAN017 and TGI ranged from -40.48% to 135.11%. Seven out of 22 PDX models responded to CAN017 with TGI ≥70% compared to controls (**Figure 2A**).

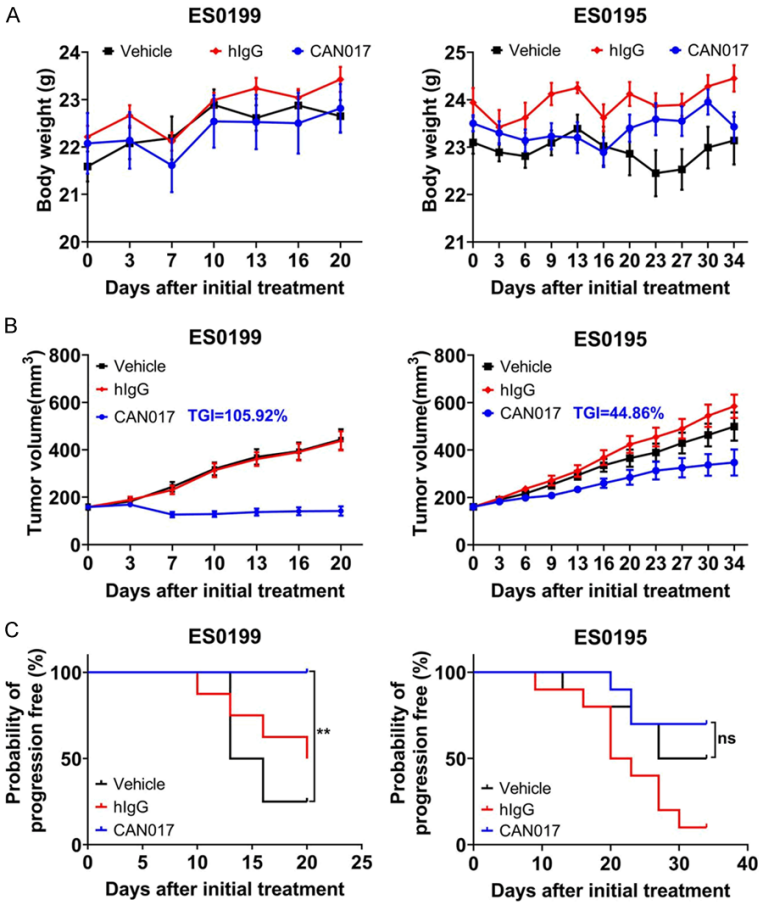


**Figure 1.** Tolerance and efficacy of CAN017 in ES0199 and ES0195 PDX models. A. Body weights of mice during treatment. Data were presented as means ± SDs. B. Tumor growth curves showed the *in vivo* activity of CAN017 in ES0199 and ES0195 PDX models treated with vehicle control, hIgG control (20 mg/kg) and CAN017 (20 mg/kg) every 3 days. Data were indicated as means ± SDs. The anti-tumor activity was depicted by TGI with 105.92% and 44.86% in ES0199 and ES0195 PDX models, respectively. C. Kaplan-Meier graph showed the probability of tumor progression-free mice in ES0199 and ES0195 PDX models during the treatment. $^{**}P < 0.01$; ns, not significant by log-rank test.

Together with the above two PDX models, 33.3% (8/24) PDX models in cohort 1 showed response to CAN017 (**Figure 2B** and Table S1). Totally, compared to hIgG control group (mean TGI: -6.23 ± 7.8%), CAN017 (mean TGI: 43.91 ± 9.6%) exerted significant anti-tumor activity ($P < 0.001$; **Figure 2C**). These results suggested that CAN017 demonstrated a very promising efficacy in ESCC.

*NRG1 rather than HER3 expression as a predictive biomarker for CAN017*

As an anti-HER3 antibody, HER3 and its predominant ligand NRG1 were focused on in this study based on the previous reported study [23]. The staining scores of HER3 and NRG1 protein expression were shown in Table S1, and neither HER3 (Pearson $R^2 = 0.13$; $P = 0.09$) nor NRG1 protein expressions (Pearson $R^2 = 0.07$; $P = 0.2$) were correlated with the efficacy of CAN017 (**Figure 3A**). Furthermore, based on RNAseq results (Table S1), there was also no obvious correlation between HER3 mRNA expression and the efficacy of CAN017 (Pearson $R^2 = 0.087$; $P = 0.16$; **Figure 3B**). However, it was very interested that higher expression of NRG1 mRNA evaluated by RNAseq was positively correlated with higher TGI of CAN017 (Pearson $R^2 = 0.37$; $P < 0.01$; **Figure 3B**). To facilitate potential clinical application, we also evaluated the NRG1 mRNA expression by RT-PCR (Table S2) and found a great correlation between RNAseq and RT-PCR for NRG1 mRNA quantification (Pearson $R^2 = 0.71$; $P < 0.001$; Figure S1A). A significantly inverse linear relationship between the NRG1 $\Delta C_t$ and the efficacy of CAN017 was found (Pearson $R^2 = 0.31$; $P < 0.01$; **Figure 3C**), which suggested that the higher NRG1 mRNA expression, the better efficacy of CAN017.

To further evaluate the potential accuracy associated with NRG1 mRNA expression in predicting CAN017 efficacy, ROC curve was performed to identify suitable NRG1 $\Delta C_t$ threshold for future screening patients (**Figure 3D**). The area under the curve (AUC) was 0.922 and a NRG1 $\Delta C_t$ threshold 7.79 point showed the maximum Yoden index (Table S3). Based on this threshold, 11 and 13 PDX models in cohort 1 were classified to NRG1-high and NRG1-low groups (Table S2), respectively, with corresponding

A

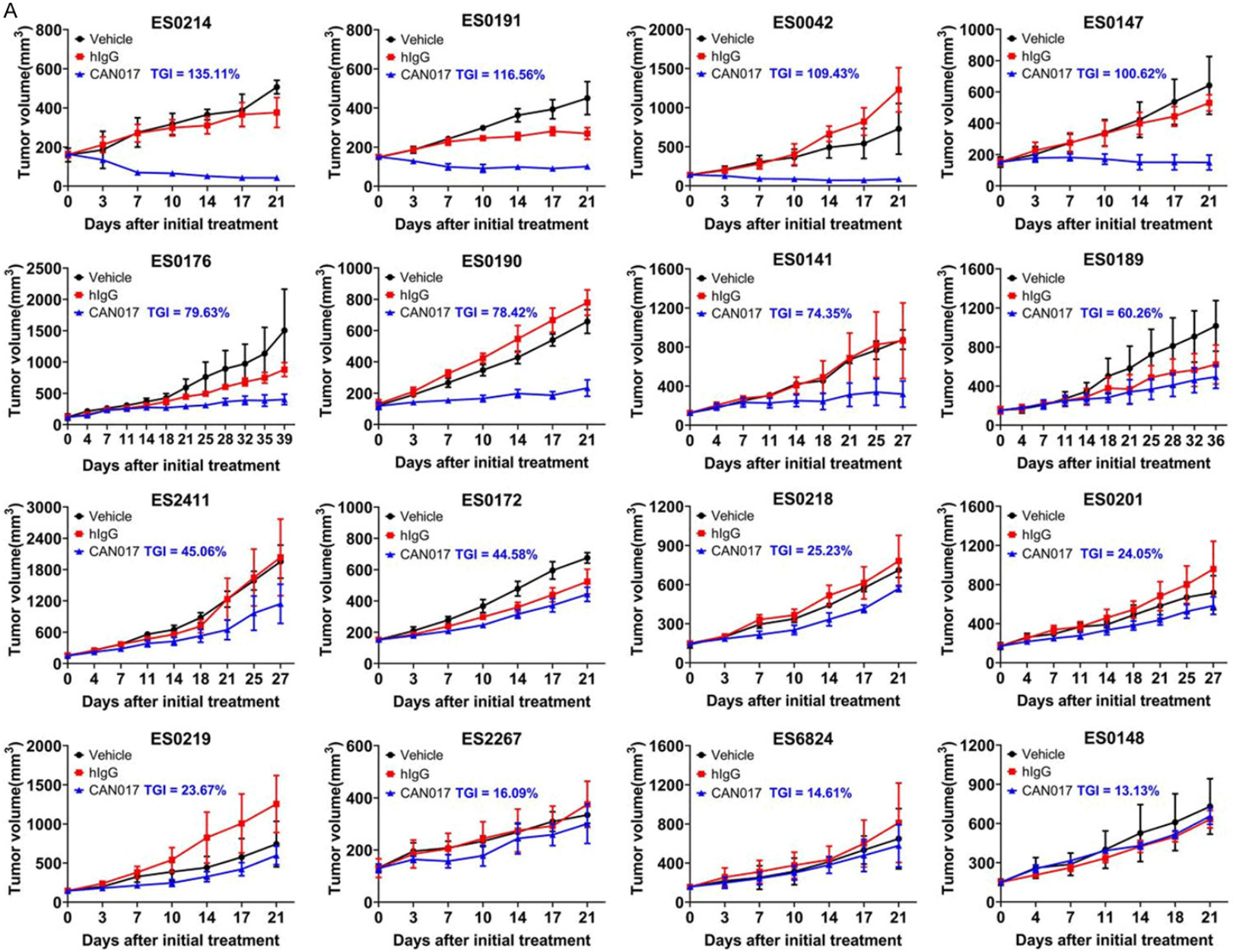
ES0214
Vehicle
hIgG
CAN017 TGI = 135.11%
Tumor volume(mm3)
Days after initial treatment
ES0191
CAN017 TGI = 116.56%
ES0042
CAN017 TGI = 109.43%
ES0147
CAN017 TGI = 100.62%
ES0176
CAN017 TGI = 79.63%
ES0190
CAN017 TGI = 78.42%
ES0141
CAN017 TGI = 74.35%
ES0189
CAN017 TGI = 60.26%
ES2411
CAN017 TGI = 45.06%
ES0172
CAN017 TGI = 44.58%
ES0218
CAN017 TGI = 25.23%
ES0201
CAN017 TGI = 24.05%
ES0219
CAN017 TGI = 23.67%
ES2267
CAN017 TGI = 16.09%
ES6824
CAN017 TGI = 14.61%
ES0148
CAN017 TGI = 13.13%

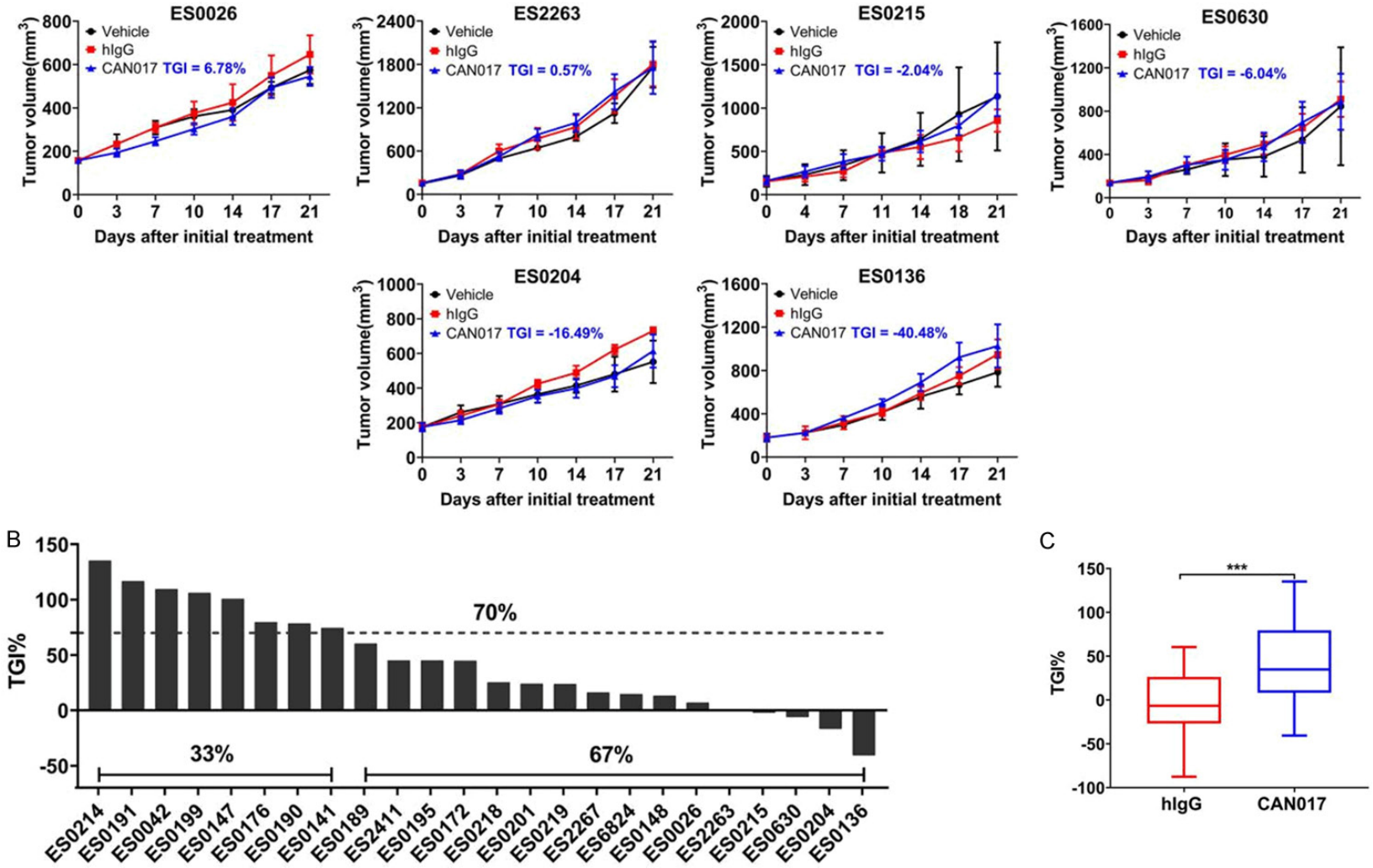


**Figure 2.** Efficacy of CAN017 in large ESCC PDX models in cohort 1. A. Tumor growth curves showed the *in vivo* activity of 22 ESCC PDX models treated with vehicle control, hIgG control (20 mg/kg) and CAN017 (20 mg/kg) every 3 days. Data were expressed as means ± SDs for at less five mice in each group. The anti-tumor activity was depicted by TGI described in each picture. B. Waterfall plot displayed the different response to CAN017 of 24 PDX models in cohort 1. Dotted line indicated the TGI of 70%. C. Comparison of tumor growth inhibition between hIgG group and CAN017 group. ***$P < 0.001$ analyzed by unpaired two-tailed *t* test.

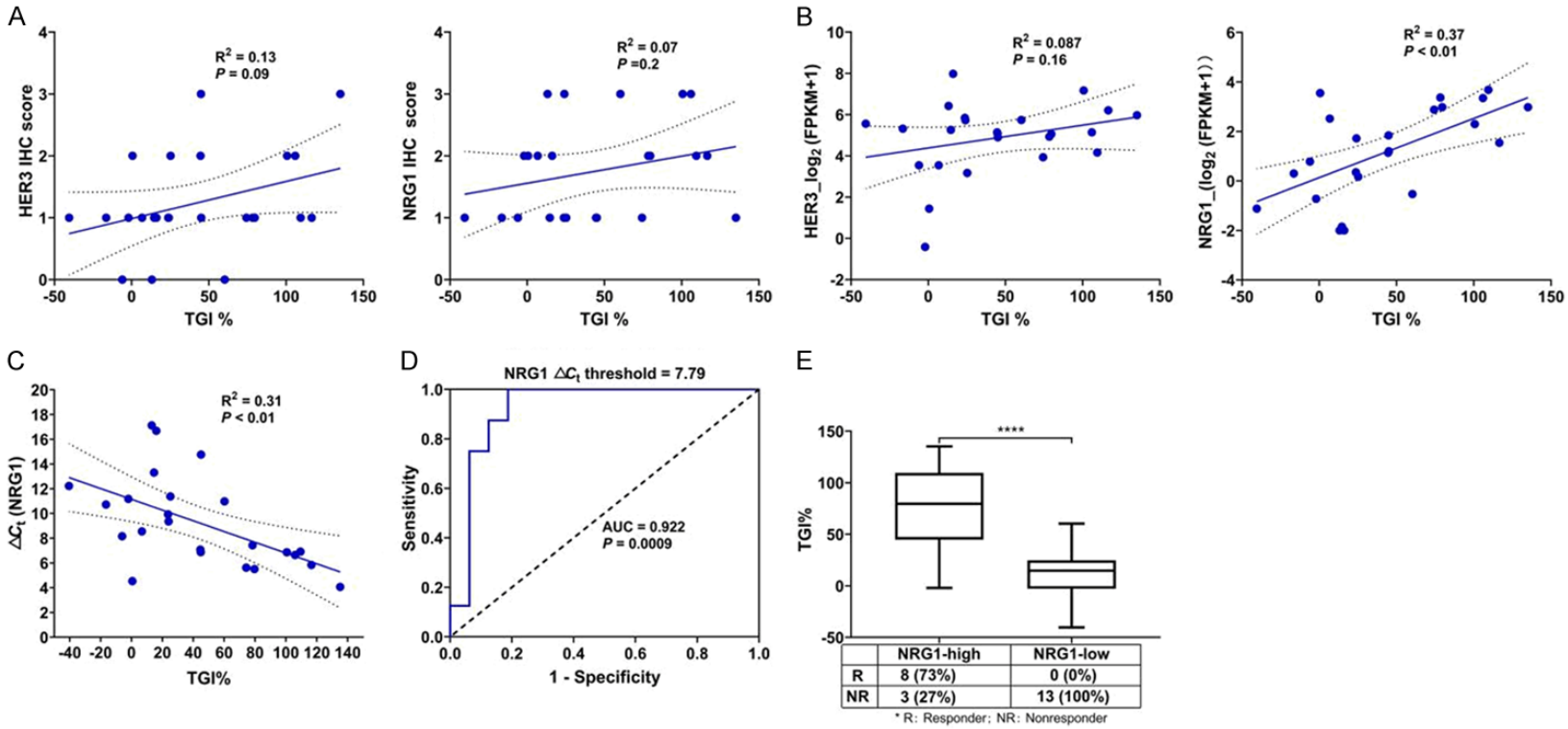


**Figure 3.** Correlation between HER3 and NRG1 expression and the efficacy of CAN017 in 24 PDX models in cohort 1. A. Pearson correlation plots of the HER3 and NRG1 protein expressions evaluated by IHC in FFPE tumors and the efficacy of CAN017 in PDX models (n = 24). The linear regression was shown by a solid line, and 95% confidence interval (CI) of the values fitted by linear regression was shown by dark dotted lines. $R^2$, the coefficient of determination. B. Pearson correlation plots of the HER3 and NRG1 mRNA expression quantified by RNAseq in tumors and the efficacy of CAN017 in PDX models (n = 24). The linear regression was shown by a solid line, and 95% CI of the values fitted by linear regression was shown by dark dotted lines. C. Pearson correlation plots of the NRG1 mRNA expression quantified by RT-PCR in FFPE tumors and the efficacy of CAN017 in PDX models (n = 24). The linear regression was shown by a solid line, and 95% CI of the values fitted by linear regression was shown by dark dotted lines. D. ROC curve analysis for the NRG1 $\Delta C_t$ threshold to predict the response of CAN017. AUC, area under curve. E. Comparison of the efficacy of CAN017 between NRG1-high and NRG1-low PDX models. ****$P < 0.0001$ analyzed by unpaired two-tailed *t* test.

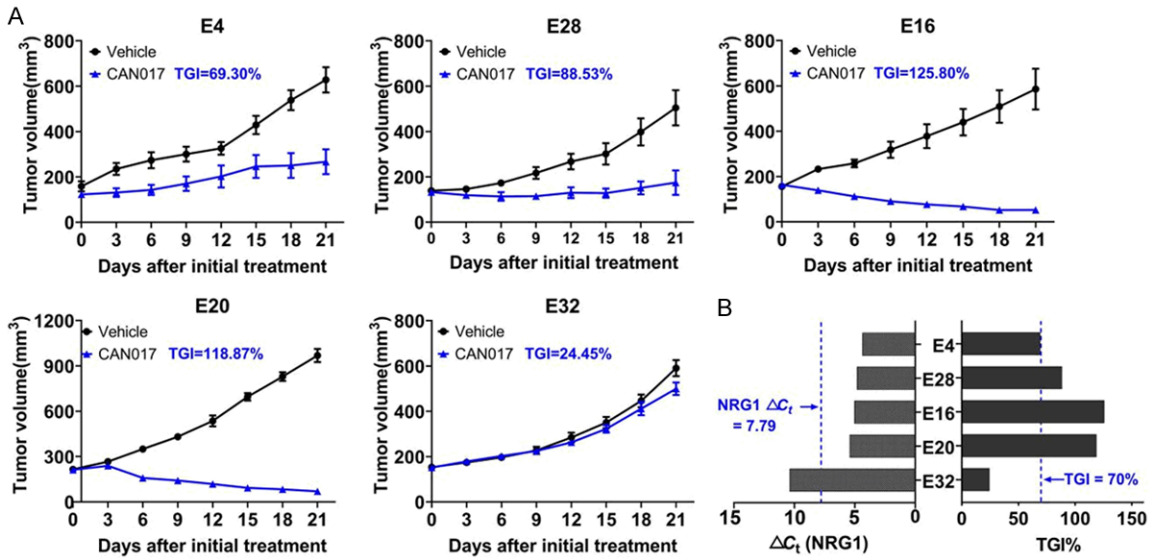


**Figure 4.** Efficacy of CAN017 prospectively guided by NRG1 expression in cohort 2. A. Tumor growth curves showed the *in vivo* activity of 5 ESCC PDX models treated with vehicle control and CAN017 (20 mg/kg). Data were expressed as means ± SDs for at less five mice in each group. The anti-tumor activity was depicted by TGI as described in each picture. B. NRG1 mRNA expression levels of 5 ESCC tumors and the efficacy of CAN017 on PDX models. Blue dotted lines showed the threshold of NRG1 $\Delta C_t$ and the TGI of 70%, respectively.

response rates were 73% versus 0% ($P < 0.0001$; **Figure 3E**).

*Validation of CAN017 efficacy guided by NRG1 expression in prospective cohort 2*

To validate the retrospective results from cohort 1, another separate cohort 2 including 22 ESCC PDX models were prospectively tested. All PDX tissues prior to CAN017 treatment were evaluated for the NRG1 mRNA expression by RT-PCR to guide model selection in subsequent biomarker-driven prospective study. Based on NRG1 expression, a total of 5 PDX models with NRG1-high (E4, E28, E16 and E20) and NRG1-low (E32, as negative control) expressions were selected to validate the efficacy of CAN017. As expected, the TGI of CAN017 in four NRG1-high models was 69.30%, 88.53%, 125.80%, and 118.87%, which were significantly higher than that in NRG1-low model (24.45%; **Figure 4A** and **4B**). Although the TGI in E4 (69.3%) with NRG1-high expression was slightly lower than 70%, the promising anti-tumor activity of CAN017 in NRG1-high expression ESCC was well worth validated in future clinical trials.

## Discussion

Chemotherapy and radiotherapy didn't show major breakthrough in the overall survival for advanced ESCC for decades, which proposed the urgent need for new drug development. In this study, we first showed the promising therapeutic potential of an anti-HER3 antibody CAN017 in ESCC PDX models which highly simulated patients and warranted the reliable results. More importantly, NRG1 mRNA expression could be used to screen suitable patients of CAN017 treatment, which was very helpful for precision therapy guided by stratified biomarkers.

HER3 is the most potent activator of the PI3K/AKT pathway among four HER receptors, and plays an essential role in tumor development, tumorigenesis and cancer progression in many tumors, such as gastric cancer, melanomas, and breast cancer [27-29]. Also, activation of HER3 was reported to be involved in resistance to anti-EGFR or anti-HER2 therapeutics [28], emphasizing the importance of developing effective agents that specifically inhibited the HER3. Several antibodies targeting HER3 had been reported to exhibit anti-tumor activity *in vivo* [30-32], however, none had been approved for clinical practice. As a novel anti-HER3 inhibitor, CAN017 demonstrated extensive preclinical anti-tumor activity in several tumors [23] and in our ESCC PDX models, and was well tolerated in a phase I study (NCT01603979) within a certain dose range [33]. All these results indicated the great potential of CAN017.

In the previous study, CAN017 demonstrated anti-tumor activity in NSCLC (non-small cell lung cancer) and head and neck tumors [25]. Therefore, 3 NSCLC and 3 head and neck PDX models from Crown Bioscience were used to detect the efficacy of CAN017 in parallel, and the results were similar with reported study (Figure S2A and S2B) [23]. In recent years, biomarker-driven targeted therapy was extremely popular and would be the main direction of future trials. Both Meetze K et al and other groups suggested NRG1 could be identified as a predictive biomarker for HER3-targeting therapy in both preclinical studies and clinical samples [23, 32, 34-37], which was also validated in our study of cohort 1 indicated as the positive correlation between NRG1 mRNA expression and CAN017's efficacy. However, a good correlation was found between NRG1 mRNA and protein expressions in 32 tumor tissues reported by Meetze K et al [23], which was not validated in our study (Pearson $R^2$ = 0.001; $P$ = 0.87; Figure S1B). The clear correlation between NRG1 mRNA and protein expressions needed to be further investigated in preclinical and clinical samples.

To facilitate the detection of NRG1 easily in future clinical trials, we also compared the NRG1 mRNA expressions in cryopreserved tumor samples and archived FFPE tumor samples. A strong correlation of NRG1 expressions between cryopreserved tumors and FFPE tumors was found (Pearson $R^2$ = 0.88; $P$ < 0.0001; Figure S1C), which ensured the feasibility of clinical NRG1 detection using easily accessible FFPE samples. Moreover, if possible, the detection methods and the cut-off criteria for NRG1 expression also needed to be optimized and defined due to the lack of standard consensus [23, 38].

It was well known that most of the targeted drugs displayed a good anti-tumor activity by combining with other drugs, such as anti-HER3 therapy combined trastuzumab in gastric cancer and anti-HER3 antibody combined cytotoxic drugs in melanoma [39, 40]. Also, we found CAN017 could overcome the secondary resistance of trastuzumab in gastric cancer PDX models (unpublished data), which was consistent with the result in breast cancer [41]. Further studies would be conducted to explore the combined strategy for CAN017 in ESCC.

In summary, this study first demonstrated that CAN017 might be a potential therapeutic drug for ESCC and highlighted the importance of NRG1 as a potential predictive marker for future clinical trials. In the following study, the combined strategy of CAN017, the role of NRG1, and the resistant mechanisms of CAN017 in ESCC would be further investigated *in vivo* and *in vitro*.

## Acknowledgements

The authors thank CANBridge Life Sciences Ltd. (Beijing, China) for providing CAN017 in this study. This study was supported by the Sanming Project of Medicine in Shenzhen, China (SZSM201812062).

## Disclosure of conflict of interest

None.

**Address correspondence to:** Lin Shen, Key Laboratory of Carcinogenesis and Translational Research (Ministry of Education/Beijing), Department of Gastrointestinal Oncology, Peking University Cancer Hospital and Institute, Fu-Cheng Road 52, Hai-Dian District, Beijing, China. Tel: +86-10-88196561; E-mail: linshenpku@163.com; Jing Gao, National Cancer Center/National Clinical Research Center for Cancer/Cancer Hospital & Shenzhen Hospital, Chinese Academy of Medical Sciences and Peking Union Medical College, No. 113 Baohe Street, Longgang District, Shenzhen, China. Tel: +86-10-13581565966; E-mail: gaojing_pumc@163.com

## References

[1] Arnold M, Soerjomataram I, Ferlay J and Forman D. Global incidence of oesophageal cancer by histological subtype in 2012. Gut 2015; 64: 381-87.

[2] Malhotra GK, Yanala U, Ravipati A, Follet M, Vijayakumar M and Are C. Global trends in esophageal cancer. J Surg Oncol 2017; 115: 564-79.

[3] Allum WH, Stenning SP, Bancewicz J, Clark PI and Langley RE. Long-term results of a randomized trial of surgery with or without preoperative chemotherapy in esophageal cancer. J Clin Oncol 2009; 27: 5062-67.

[4] Medical Research Council Oesophageal Cancer Working Group. Surgical resection with or without preoperative chemotherapy in oesoph-

ageal cancer: a randomised controlled trial. Lancet 2002; 359: 1727-33.
[5] Siegel R, Ma J, Zou Z and Jemal A. Cancer statistics, 2014. CA Cancer J Clin 2014; 64: 9-29.
[6] Waddell T, Chau I, Cunningham D, Gonzalez D, Okines AF, Okines C, Wotherspoon A, Saffery C, Middleton G, Wadsley J, Ferry D, Mansoor W, Crosby T, Coxon F, Smith D, Waters J, Iveson T, Falk S, Slater S, Peckitt C and Barbachano Y. Epirubicin, oxaliplatin, and capecitabine with or without panitumumab for patients with previously untreated advanced oesophagogastric cancer (REAL3): a randomised, open-label phase 3 trial. Lancet Oncol 2013; 14: 481-9.
[7] Dutton SJ, Ferry DR, Blazeby JM, Abbas H, Dahle-Smith A, Mansoor W, Thompson J, Harrison M, Chatterjee A, Falk S, Garcia-Alonso A, Fyfe DW, Hubner RA, Gamble T, Peachey L, Davoudianfar M, Pearson SR, Julier P, Jankowski J, Kerr R and Petty RD. Gefitinib for oesophageal cancer progressing after chemotherapy (COG): a phase 3, multicentre, double-blind, placebo-controlled randomised trial. Lancet Oncol 2014; 15: 894-904.
[8] Suntharalingam M, Winter K, Ilson D, Dicker AP, Kachnic L, Konski A, Chakravarthy AB, Anker CJ, Thakrar H, Horiba N, Dubey A, Greenberger JS, Raben A, Giguere J, Roof K, Videtic G, Pollock J, Safran H and Crane CH. Effect of the addition of cetuximab to paclitaxel, cisplatin, and radiation therapy for patients with esophageal cancer: the NRG oncology RTOG 0436 phase 3 randomized clinical trial. JAMA Oncol 2017; 3: 1520-28.
[9] Ilson DH, Kelsen D, Shah M, Schwartz G, Levine DA, Boyd J, Capanu M, Miron B and Klimstra D. A phase 2 trial of erlotinib in patients with previously treated squamous cell and adenocarcinoma of the esophagus. Cancer 2011; 117: 1409-14.
[10] Lu M, Wang X, Shen L, Jia J, Gong J, Li J, Li J, Li Y, Zhang X, Lu Z, Zhou J and Zhang X. Nimotuzumab plus paclitaxel and cisplatin as the first line treatment for advanced esophageal squamous cell cancer: a single centre prospective phase II trial. Cancer Sci 2016; 107: 486-90.
[11] Berger MB, Mendrola JM and Lemmon MA. ErbB3/HER3 does not homodimerize upon neuregulin binding at the cell surface. FEBS Lett 2004; 569: 332-36.
[12] Burgess AW, Cho HS, Eigenbrot C, Ferguson KM, Garrett TP, Leahy DJ, Lemmon MA, Sliwkowski MX, Ward CW and Yokoyama S. An open-and-shut case? Recent insights into the activation of EGF_ErbB receptors. Mol Cell 2003; 12: 541-52.
[13] Holbro T, Beerli RR, Maurer F, Koziczak M, Barbas CR and Hynes NE. The ErbB2/ErbB3 heterodimer functions as an oncogenic unit: ErbB2 requires ErbB3 to drive breast tumor cell proliferation. Proc Natl Acad Sci U S A 2003; 100: 8933-8.
[14] Crovello CS, Lai C, Cantley LC and Carraway KL. Differential signaling by the epidermal growth factor-like growth factors neuregulin-1 and neuregulin-2. J Biol Chem 1998; 273: 26954-61.
[15] Shames DS, Carbon J, Walter K, Jubb AM, Kozlowski C, Januario T, Do A, Fu L, Xiao Y, Raja R, Jiang B, Malekafzali A, Stern H, Settleman J, Wilson TR, Hampton GM, Yauch RL, Pirzkall A and Amler LC. High heregulin expression is associated with activated HER3 and may define an actionable biomarker in patients with squamous cell carcinomas of the head and neck. PLoS One 2013; 8: e56765.
[16] Wilson TR, Lee DY, Berry L, Shames DS and Settleman J. Neuregulin-1-mediated autocrine signaling underlies sensitivity to HER2 kinase inhibitors in a subset of human cancers. Cancer Cell 2011; 20: 158-72.
[17] Kawakami H, Okamoto I, Yonesaka K, Okamoto K, Shibata K, Shinkai Y, Sakamoto H, Kitano M, Tamura T, Nishio K and Nakagawa K. The anti-HER3 antibody patritumab abrogates cetuximab resistance mediated by heregulin in colorectal cancer cells. Oncotarget 2014; 5: 11847-56.
[18] Yun S, Koh J, Nam SK, Park JO, Lee SM, Lee K, Lee KS, Ahn SH, Park DJ, Kim HH, Choe G, Kim WH and Lee HS. Clinical significance of overexpression of NRG1 and its receptors, HER3 and HER4, in gastric cancer patients. Gastric Cancer 2018; 21: 225-36.
[19] Kolb A, Kleeff J, Arnold N, Giese NA, Giese T, Korc M, Korc M and Friess H. Expression and differential signaling of heregulins in pancreatic cancer cells. Int J Cancer 2007; 120: 514-23.
[20] Qian G, Jiang N, Wang D, Newman S, Kim S, Chen Z, Garcia G, MacBeath G, Shin DM, Khuri FR, Chen ZG and Saba NF. Heregulin and HER3 are prognostic biomarkers in oropharyngeal squamous cell carcinoma. Cancer 2015; 121: 3600-11.
[21] Yamamoto Y, Yamai H, Seike J, Yoshida T, Takechi H, Furukita Y, Koichiro K, Takuya M, Yoshimi B and Akira T. Prognosis of esophageal squamous cell carcinoma in patients positive for human epidermal growth factor receptor family can be improved by initial chemotherapy with docetaxel, fluorouracil, and cisplatin. Ann Surg Oncol 2012; 19: 757-65.
[22] Vincent S, Fleet C, Bottega S, Mcintosh D, Winston W and Chen T. Abstract 2509: AV-203, a humanized ERBB3 inhibitory antibody inhibits

ligand-dependent and ligand-independent ERBB3 signaling in vitro and in vivo. Cancer Res 2012; 72 Suppl: 2509.

[23] Meetze K, Vincent S, Tyler S, Mazsa EK, Delpero AR, Bottega S, McIntosh D, Nicoletti R, Winston WM, Weiler S, Feng B, Gyuris J and Weng Z. Neuregulin 1 expression is a predictive biomarker for response to AV-203, an ERBB3 inhibitory antibody, in human tumor models. Clin Cancer Res 2015; 21: 1106-14.

[24] Zou J, Liu Y, Wang J, Liu Z, Lu Z, Chen Z, Li Z, Dong B, Huang W, Li Y, Gao J and Shen L. Establishment and genomic characterizations of patient-derived esophageal squamous cell carcinoma xenograft models using biopsies for treatment optimization. J Transl Med 2018; 16: 15.

[25] Liu Z, Chen Z, Wang J, Zhang M, Li Z, Wang S, Dong B, Zhang C, Gao J and Shen L. Mouse avatar models of esophageal squamous cell carcinoma proved the potential for EGFR-TKI afatinib and uncovered Src family kinases involved in acquired resistance. J Hematol Oncol 2018; 11: 109.

[26] Rüschoff J, Dietel M, Baretton G, Arbogast S, Walch A, Monges G, Chenard MP, Penault-Llorca F, Nagelmeier I, Schlake W, Höfler H and Kreipe HH. HER2 diagnostics in gastric cancer-guideline validation and development of standardized immunohistochemical testing. Virchows Arch 2010; 457: 299-307.

[27] Ocana A, Vera-Badillo F, Seruga B, Templeton A, Pandiella A and Amir E. HER3 overexpression and survival in solid tumors: a meta-analysis. J Natl Cancer Inst 2013; 105: 266-73.

[28] Amin DN, Campbell MR and Moasser MM. The role of HER3, the unpretentious member of the HER family, in cancer biology and cancer therapeutics. Semin Cell Dev Biol 2010; 21: 944-50.

[29] Ocana A, Vera-Badillo F, Seruga B, Templeton A, Pandiella A and Amir E. HER3 overexpression and survival in solid tumors: a meta-analysis. J Natl Cancer Inst 2013; 105: 266-73.

[30] Bourillon L, Demontoy S, Lenglet A, Zampieri A, Fraisse J, Jarlier M, Boissière-Michot F, Perrochia H, Rathat G, Garambois V, Bonnefoy N, Michaud HA, Chardès T, Tosi D, Pèlegrin A, Azria D, Larbouret C and Bourgier C. Higher Anti-Tumor efficacy of the dual HER3-EGFR antibody MEHD7945a combined with ionizing irradiation in cervical cancer cells. Int J Radiat Oncol Biol Phys 2020; 106: 1039-51.

[31] Jacob W, James I, Hasmann M and Weisser M. Clinical development of HER3-targeting monoclonal antibodies: perils and progress. Cancer Treat Rev 2018; 68: 111-23.

[32] Schoeberl B, Kudla A, Masson K, Kalra A, Curley M, Finn G, Pace E, Harms B, Kim J, Kearns J, Fulgham A, Burenkova O, Grantcharova V, Yarar D, Paragas V, Fitzgerald J, Wainszelbaum M, West K, Mathews S, Nering R, Adiwijaya B, Garcia G, Kubasek B, Moyo V, Czibere A, Nielsen UB and MacBeath G. Systems biology driving drug development: from design to the clinical testing of the anti-ErbB3 antibody seribantumab (MM-121). NPJ Syst Biol Appl 2017; 3: 16034.

[33] Sarantopoulos J, Gordon MS, Harvey RD, Sankhala KK, Malik L, Mahalingam D, Owonikoko TK, Lewis CM, Payumo F, Miller J, Powell C, Weng Z and Komarnitsky PB and Ramalingam SS. Abstract 11113: first-in-human phase 1 dose-escalation study of AV-203, a monoclonal antibody against ERBB3, in patients with metastatic or advanced solid tumors. J Clin Oncol 2014; 32 Suppl: 11113.

[34] Schoeberl B, Faber AC, Li D, Liang MC, Crosby K, Onsum M, Burenkova O, Pace E, Walton Z, Nie L, Fulgham A, Song Y, Nielsen UB, Engelman JA and Wong KK. An ErbB3 antibody, MM-121, is active in cancers with ligand-dependent activation. Cancer Res 2010; 70: 2485-94.

[35] Kawakami H, Okamoto I, Yonesaka K, Okamoto K, Shibata K, Shinkai Y, Sakamoto H, Kitano M, Tamura T, Nishio K and Nakagawa K. The anti-HER3 antibody patritumab abrogates cetuximab resistance mediated by heregulin in colorectal cancer cells. Oncotarget 2014; 5: 11847-56.

[36] Shames DS, Carbon J, Walter K, Jubb AM, Kozlowski C, Januario T, Do A, Fu L, Xiao Y, Raja R, Jiang B, Malekafzali A, Stern H, Settleman J, Wilson TR, Hampton GM, Yauch RL, Pirzkall A and Amler LC. High heregulin expression is associated with activated HER3 and may define an actionable biomarker in patients with squamous cell carcinomas of the head and neck. PLoS One 2013; 8: e56765.

[37] Wilson TR, Lee DY, Berry L, Shames DS and Settleman J. Neuregulin-1-mediated autocrine signaling underlies sensitivity to HER2 kinase inhibitors in a subset of human cancers. Cancer Cell 2011; 20: 158-72.

[38] Qian G, Jiang N, Wang D, Newman S, Kim S, Chen Z, Garcia G, MacBeath G, Shin DM, Khuri FR, Chen ZG and Saba NF. Heregulin and HER3 are prognostic biomarkers in oropharyngeal squamous cell carcinoma. Cancer 2015; 121: 3600-11.

[39] Wang Q, Zhang X, Shen E, Gao J, Cao F, Wang X, Li Y, Tian T, Wang J, Chen Z, Wang J and Shen L. The anti-HER3 antibody in combina-

tion with trastuzumab exerts synergistic antitumor activity in HER2-positive gastric cancer. Cancer Lett 2016; 380: 20-30.

[40] Capone E, Lamolinara A, D'Agostino D, Rossi C, De Laurenzi V, Iezzi M, Angelucci F, Sorda R, Laurenzi V, Natali PG, Ippoliti R, Iacobelli S and Sala G. EV20-mediated delivery of cytotoxic auristatin MMAF exhibits potent therapeutic efficacy in cutaneous melanoma. J Control Release 2018; 277: 48-56.

[41] Huang J, Wang S, Lyu H, Cai B, Yang X, Wang J and Liu B. The anti-erbB3 antibody MM-121/SAR256212 in combination with trastuzumab exerts potent antitumor activity against trastuzumab-resistant breast cancer cells. Mol Cancer 2013; 12: 134.

**Table S1.** Summary of the efficacy of CAN017, HER3 and NRG1 expressions on PDX models of cohort 1

| PDX model ID | TGI (%) | HER3 IHC score | NRG1 IHC score | HER3 RNAseq ($log_2$ (FPKM+1)) | NRG1 RNAseq ($log_2$ (FPKM+1)) |
|---|---|---|---|---|---|
| ES0214 | 135.11 | 3+ | 1+ | 5.97 | 2.98 |
| ES0191 | 116.56 | 1+ | 2+ | 6.21 | 1.54 |
| ES0042 | 109.43 | 1+ | 2+ | 4.16 | 3.68 |
| ES0199 | 105.92 | 3+ | 3+ | 5.14 | 3.35 |
| ES0147 | 100.62 | 2+ | 3+ | 7.17 | 2.3 |
| ES0176 | 79.63 | 1+ | 2+ | 5.06 | 2.98 |
| ES0190 | 78.42 | 1+ | 2+ | 4.93 | 3.37 |
| ES0141 | 74.35 | 1+ | 1+ | 3.93 | 2.88 |
| ES0189 | 60.26 | 1+ | 3+ | 5.74 | -0.53 |
| ES2411 | 45.06 | 1+ | 1+ | 4.9 | 1.2 |
| ES0195 | 44.86 | 3+ | 1+ | 5.08 | 1.84 |
| ES0172 | 44.58 | 2+ | 1+ | 5.14 | 1.14 |
| ES0218 | 25.23 | 2+ | 1+ | 3.17 | 0.17 |
| ES0201 | 24.05 | 1+ | 3+ | 5.73 | 1.72 |
| ES0219 | 23.67 | 1+ | 1+ | 5.84 | 0.35 |
| ES2267 | 16.09 | 1+ | 2+ | 7.98 | -2 |
| ES6824 | 14.61 | 1+ | 1+ | 5.26 | -1.85 |
| ES0148 | 13.13 | 0 | 3+ | 6.42 | -2 |
| ES0026 | 6.78 | 1+ | 2+ | 3.54 | 2.52 |
| ES2263 | 0.57 | 2+ | 2+ | 1.44 | 3.55 |
| ES0215 | -2.04 | 1+ | 2+ | -0.42 | -0.72 |
| ES0630 | -6.04 | 0 | 1+ | 3.54 | 0.78 |
| ES0204 | -16.49 | 1+ | 1+ | 5.32 | 0.3 |
| ES0136 | -40.48 | 1+ | 1+ | 5.56 | -1.12 |

**Table S2.** Summary of NRG1 expressions evaluated by RT-PCR on 11 NRG1-high and 13 NRG1-low PDX models of cohort 1

| Groups | PDX model ID | $\Delta C_t$ (NRG1) |
|---|---|---|
| NRG1-high | ES0214 | 4.05848333 |
| | ES2263 | 4.536124333 |
| | ES0176 | 5.505088333 |
| | ES0141 | 5.618715 |
| | ES0191 | 5.837773667 |
| | ES0199 | 6.643713333 |
| | ES0147 | 6.866417 |
| | ES0195 | 6.874196 |
| | ES0042 | 6.914877333 |
| | ES0172 | 7.077805333 |
| | ES0190 | 7.426407667 |
| NRG1-low | ES0630 | 8.162932333 |
| | ES0026 | 8.552053 |
| | ES0201 | 9.356858333 |
| | ES0219 | 9.935386333 |
| | ES0204 | 10.724936 |

| | |
|---|---|
| ES0189 | 10.98290967 |
| ES0215 | 11.179748 |
| ES0218 | 11.378266 |
| ES0136 | 12.225814 |
| ES6824 | 13.306448 |
| ES2411 | 14.76201567 |
| ES2267 | 16.686158 |
| ES0148 | 17.12613767 |

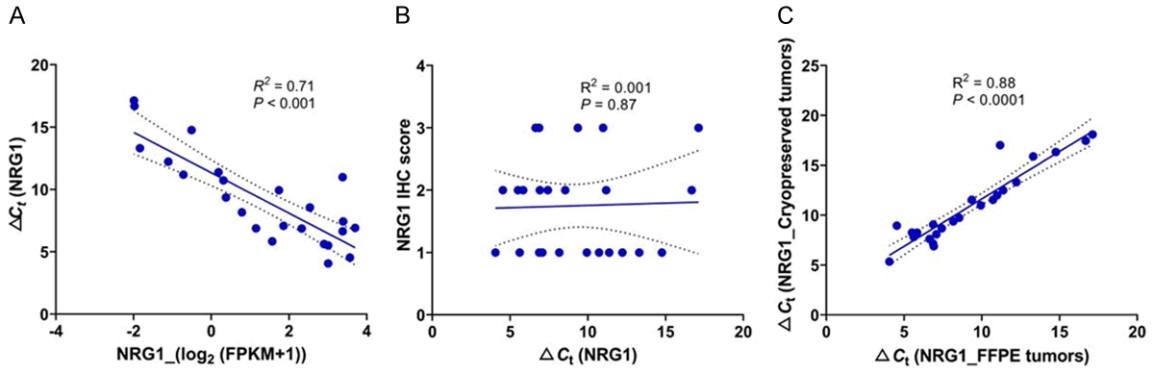


**Figure S1.** NRG1 expressions in tumor samples prior to treatment in cohort 1. A. Pearson correlation plots of the NRG1 mRNA expression detected by RNAseq and RT-PCR in PDX tumors (n = 24). B. Pearson correlation of the NRG1 mRNA and protein expressions in FFPE tumors (n = 24). C. Pearson correlation of the NRG1 mRNA expression in cryopreserved tumors and paired FFPE tumors. The linear regression was shown by a solid line, and 95% confidence interval (CI) of the values fitted by linear regression was shown by dark dotted lines. $R^2$, the coefficient of determination.

**Table S3.** The data of AUC curves for analyzing the threshold of NRG1 $\Delta C_t$

| Positive if less than or equal to[a] | Sensitivity | 1-Specificity | Yoden Index[b] |
|---|---|---|---|
| 3.0585 | 0 | 0 | 0 |
| 4.2973 | 0.125 | 0 | 0.125 |
| 5.0206 | 0.125 | 0.063 | 0.062 |
| 5.5619 | 0.25 | 0.063 | 0.187 |
| 5.7282 | 0.375 | 0.063 | 0.312 |
| 6.2407 | 0.5 | 0.063 | 0.437 |
| 6.7551 | 0.625 | 0.063 | 0.562 |
| 6.8703 | 0.75 | 0.063 | 0.687 |
| 6.8945 | 0.75 | 0.125 | 0.625 |
| 6.9963 | 0.875 | 0.125 | 0.75 |
| 7.2521 | 0.875 | 0.188 | 0.687 |
| **7.7947** | **1** | **0.188** | **0.812** |
| 8.3575 | 1 | 0.25 | 0.75 |
| 8.9545 | 1 | 0.313 | 0.687 |
| 9.6461 | 1 | 0.375 | 0.625 |
| 10.3302 | 1 | 0.438 | 0.562 |
| 10.8539 | 1 | 0.5 | 0.5 |
| 11.0813 | 1 | 0.563 | 0.437 |
| 11.279 | 1 | 0.625 | 0.375 |

| | | | |
|---|---|---|---|
| 11.802 | 1 | 0.688 | 0.312 |
| 12.7661 | 1 | 0.75 | 0.25 |
| 14.0342 | 1 | 0.813 | 0.187 |
| 15.7241 | 1 | 0.875 | 0.125 |
| 16.9061 | 1 | 0.938 | 0.062 |
| 18.1261 | 1 | 1 | 0 |

[a]The smallest cut-off value was the minimum observed test value minus 1, and the largest cut-off value was the maximum observed test value plus 1. All the other cut-off values were the averages of two consecutive ordered observed test values. [b]Yoden Index = Sensitivity-(1-specificity). A threshold with the maximum Yoden index meaned the optimal threshold (Shown in bold).

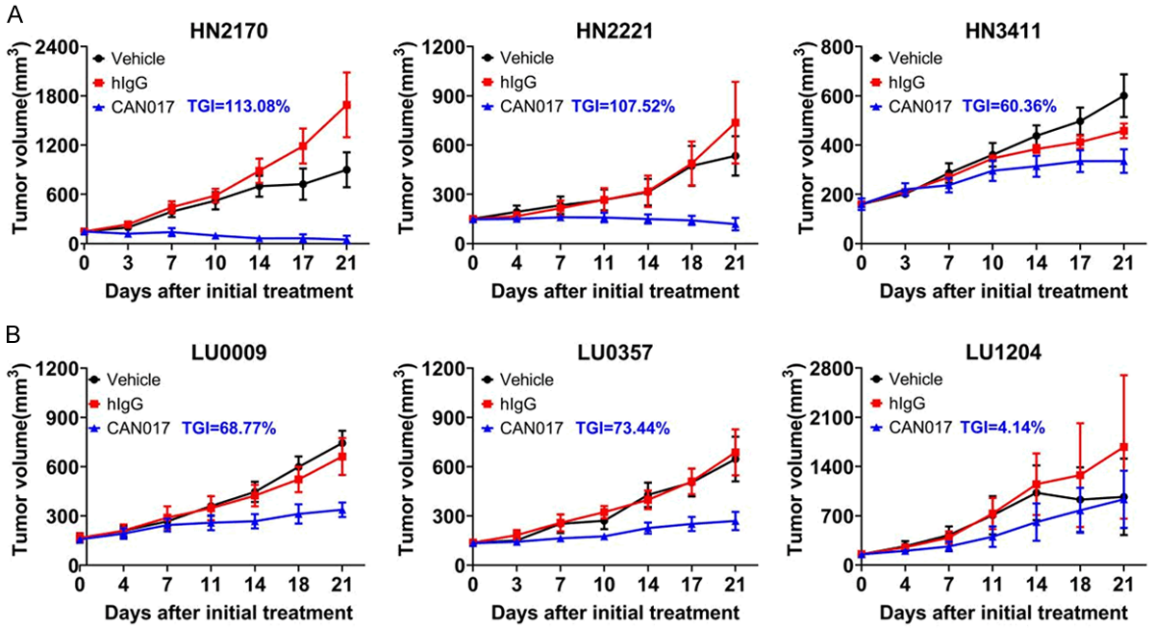


**Figure S2.** Efficacy of CAN017 on PDX models derived from head and neck cancer and NSCLC. A. Tumor growth curves showed the *in vivo* activity of CAN017 in 3 head and neck cancer PDX models. B. Tumor growth curves showed the *in vivo* activity of CAN017 in 3 NSCLC PDX models. Mice were randomized and treated with vehicle control, hIgG control (20 mg/kg) and CAN017 (20 mg/kg) when tumor volume reached approximately 150 $mm^3$. The anti-tumor activity was depicted by TGI described in each picture. Data were presented as means ± SDs.